

Photophysical studies of 1,4-diazabicyclo(2,2,2)octane as a bifunctional ligand to fix the conformation of a flexibly-linked phorbinate-zinc dimer

E.-L. Puranen^a, M.E. Stapelbroek-Möllmann^a, E. Vuorimaa^{a,*}, N. Tkachenko^a,
A.Y. Tauber^{a,b}, P.H. Hynninen^b, H. Lemmetyinen^a

^a Institute of Materials Chemistry, Tampere University of Technology, P.O. Box 541, Fin-33101 Tampere, Finland

^b Laboratory of Organic Chemistry, Department of Chemistry, University of Helsinki, P.O. Box 55, Fin-00014 Helsinki, Finland

Received 13 April 2000; received in revised form 31 July 2000; accepted 2 August 2000

Abstract

The binding of a bifunctional ligand 1,4-diazabicyclo(2,2,2)octane (DABCO) to a phorbin-dimer (PP) in which a phytychlorin is covalently linked with a flexible spacer to a modified phytyl residue of pyropheophytin was studied in order to establish a rigid face-to-face intramolecular dimer. Steady-state and time-resolved fluorescence and absorption spectroscopies were employed to characterize the binding equilibrium in CH₂Cl₂ and to verify the formation of a 1:1 complex where DABCO is bound between the Zn-phorbin rings of the dimer. The proportion of this complex is highest, about 88%, at the molar ratio of ligand:substrate = 1.5:1 while at higher molar ratios, a second DABCO molecule binds to the dimer breaking down the fixed complex. © 2000 Elsevier Science S.A. All rights reserved.

Keywords: 1,4-Diazabicyclo(2,2,2)octane; Phorbin-dimer; Complexation; Fluorescence

1. Introduction

Recently we reported the synthesis and characterization of new TRIAD molecules (Fig. 1) [1,2]. In these TRIADs, a phytychlorin-antraquinone dyad is covalently linked to the modified phytyl residue of pyropheophytin *a* with a flexible linkage leaving a substantial degree of conformational freedom in the system. The photochemical properties of these TRIADs were found to be complicated, since the flexible spacer group between the donor groups allows a variety of conformers to exist simultaneously.

Intermolecular interaction and complexation play an important role in many chemical and biological processes. Zinc-porphyrins and -pheophorbides generally bind a single ligand such as pyridine to form a five-coordinate species [3–6]. Thus, in pyridine solution zinc-pheophorbides are fully complexed yielding a characteristic sharp, intense and red-shifted absorption. To study the possibility to fix the macrocycles of the TRIAD into an ordered complex, the corresponding flexibly-linked phorbin-dimer (PP) and its zinc-complex (Zn₂PP) were synthesized. The coordination reactions of the dimer, Zn₂PP, and those of the corresponding monomer, 13²-demethoxycarbonylphorbinate-zinc(II),

ZnP_{Phy} with a bifunctional ligand 1,4-diazabicyclo(2,2,2)octane (DABCO) (Fig. 1) were studied in this work. The predicted conformation of Zn₂PP complexed with DABCO is mainly face-to-face with respect to the two macrocycles. The DABCO coordinates strongly with the central zinc atom, preventing specific association between the chromophores but several forms of coordination complexes can coexist [3–5]. To elucidate the fashion in which DABCO coordinates to Zn₂PP, the results were compared with those obtained by using pyridine as a monofunctional ligand.

2. Experimental section

13²-Demethoxycarbonylphoeophytin *a* (pyropheophytin *a*) (P_{Phy}) and the covalently-linked phorbin-dimers 3¹,3²-didehydrophytychlorin (13²-demethoxycarbonylphoeophytin *a*-P4 (*R,S*-yl) ester (PP1,2) were prepared as described elsewhere [7,8]. Dichloromethane (Merck, 99.5%), and pyridine (J.T. Baker >99.5%) were dried with type 3 or 4 Å molecular sieves and used without further purification. The DABCO (>97%) was purchased from Aldrich and used without further purification.

The behavior of the epimers PP1 and PP2 in various solvents was found to be similar. Thus, in the present study, only the epimer PP2 was used and is, henceforth, referred to as PP.

* Corresponding author. Tel.: +358-3-365-2333; fax: +358-3-365-2108.
E-mail address: vuorimaa@butler.cc.tut.fi (E. Vuorimaa).

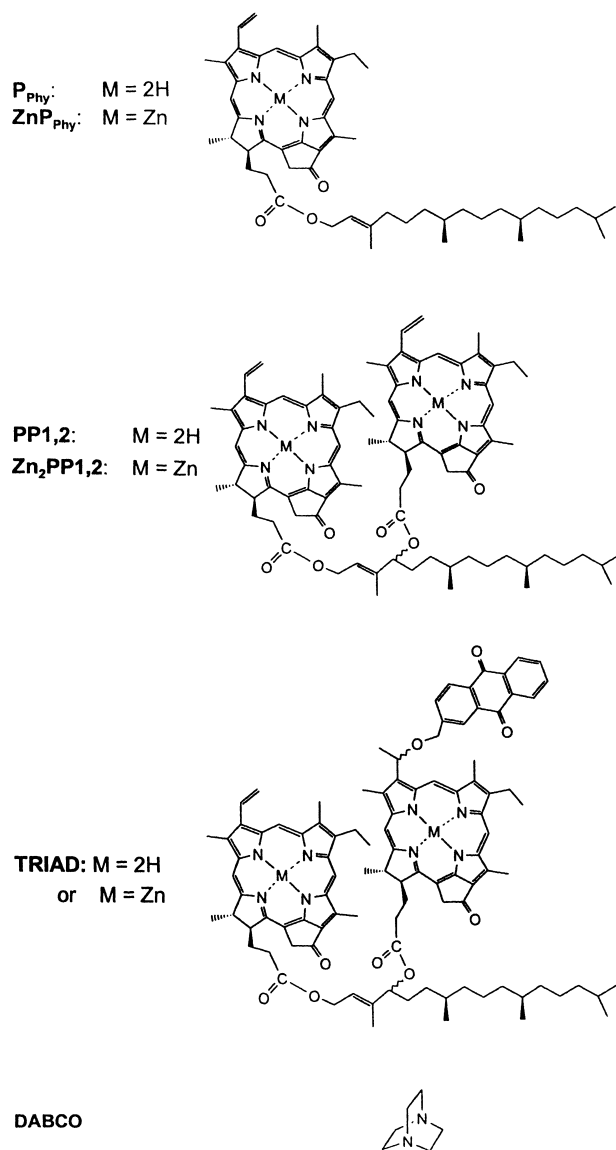


Fig. 1. Structures of the studied molecules.

Insertion of zinc(II) into the PP and P_{Phy} was accomplished according to the standard procedure [9] by refluxing the chloroform solution of the corresponding metal-free derivative with a five-fold excess of Zn(II)-acetate in methanol. The metallation yielded quantitatively the Zn(II)-complexes of the dimer PP and its reference compound P_{Phy} . In the titration experiments, the ligands were added to the CH_2Cl_2 solutions with a microliter syringe to achieve the required ligand:substrate ratio. The molarities of ZnP_{Phy} and Zn_2PP in the samples were adjusted to $2 \mu M$.

The absorption spectra were measured by a Shimadzu UV-2501PC spectrophotometer and the steady-state fluorescence spectra by a SPEX Fluorolog 3 spectrofluorometer. The fluorescence decay curves were recorded with a time-correlated single-photon-counting system (Edinburgh Instrument 199) as described previously [10]. The samples were excited by 20 ps pulses at the wavelength of 590 nm

and the response time of the instrument set-up was about 100 ps. The fluorescence decay curves were recorded at 660 nm. To diminish the influence of the scattered excitation, a red cut-off filter was used in front of the monochromator. The instrumental response function was measured separately and the fluorescence kinetic curves were deconvoluted and analyzed by the iterative least-squares method fitting with one- and two-exponential fits. Only fittings with weighted mean-square deviation, χ^2 , better than 1.2 were considered successful.

3. Results

Absorption spectra of $2 \mu M$ ZnP_{Phy} and Zn_2PP in CH_2Cl_2 and in pyridine are shown in Fig. 2. In pyridine solution, ZnP_{Phy} and Zn_2PP are fully complexed yielding characteristic sharp, intense and red-shifted absorption bands. The $2 \mu M$ solutions of ZnP_{Phy} and Zn_2PP in CH_2Cl_2 were titrated with pyridine and the changes in the absorption spectra were monitored. With increasing pyridine concentration, the absorption spectra of both ZnP_{Phy} and Zn_2PP approached the spectra observed in neat pyridine: the absorption intensities increased and the absorption maxima shifted to the red (Fig. 2). Quite large amounts of pyridine, corresponding to a value of 100:1 for the molar ratio of ligand:substrate were needed to reach the saturation level. When ZnP_{Phy} in CH_2Cl_2 was titrated with DABCO, comparable changes were observed but the saturation level was

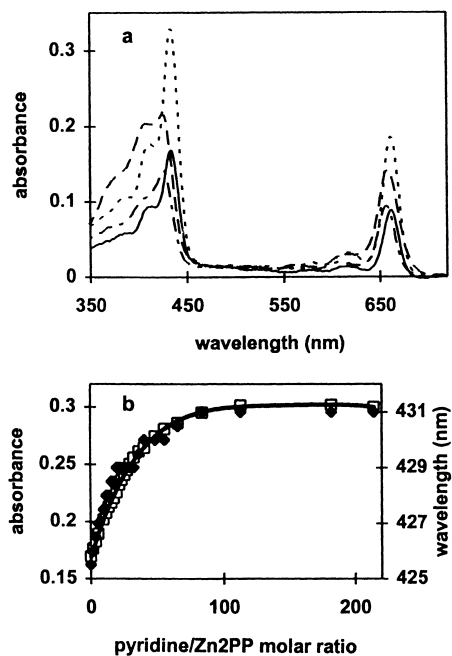


Fig. 2. (a) Absorption spectra of $2 \mu M$ solutions of ZnP_{Phy} in pyridine (—), and in CH_2Cl_2 (---); Zn_2PP in pyridine (•••) and in CH_2Cl_2 (-•-•). (b) Changes in the Soret-band in CH_2Cl_2 as a function of the pyridine: Zn_2PP molar ratio: absorption maximum wavelength (◆) and absorbance at 431 nm (□).

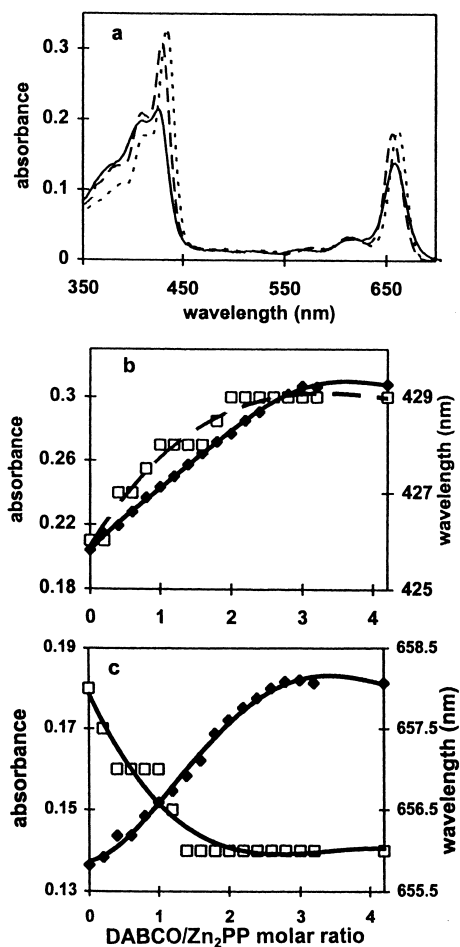


Fig. 3. (a) Absorption spectra of Zn₂PP in CH₂Cl₂ in the presence of DABCO: DABCO:Zn₂PP molar ratio 0:1 (—), and 5:1 (---); Zn₂PP in neat pyridine (● ● ●). (b) Changes in the Soret-band in CH₂Cl₂ as a function of the DABCO:Zn₂PP molar ratio: absorption maximum wavelength (□) and absorbance at 429 nm (◆). (c) Changes in the Q-band in CH₂Cl₂ as a function of DABCO:Zn₂PP molar ratio: absorption maximum wavelength (□) and absorbance at 656 nm (◆).

obtained already at the molar ratio DABCO:ZnP_{phy} = 6:1. Titrating Zn₂PP with DABCO in CH₂Cl₂, the Soret-band shifted to the red but for the Q-band a blue shift was observed (Fig. 3). Again a very small amount of DABCO was needed to reach the saturation level. For the changes in the absorption intensities at 429 and 656 nm, saturation was reached at the molar ratio DABCO:Zn₂PP = 3:1 whereas for the shifts in the absorption maxima, saturation was reached already at the molar ratio DABCO:Zn₂PP = 2:1.

The fluorescence quantum yields of the 2 μM solutions of Zn₂PP, calculated relative to ZnP_{phy} were 0.25 ± 0.05 and 0.73 ± 0.05 in CH₂Cl₂ and pyridine, respectively. With increasing DABCO concentration, the relative fluorescence quantum yield of Zn₂PP in CH₂Cl₂ increased to 0.71 ± 0.05 at the molar ratio DABCO:Zn₂PP = 1.5:1, and then decreased to 0.63 ± 0.05 with a further increase in DABCO concentration (Fig. 4). For ZnP_{phy} in CH₂Cl₂, the fluorescence efficiency increased only slightly: at the molar

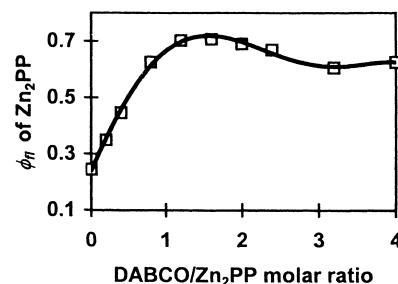


Fig. 4. Relative fluorescence quantum yield, ϕ_f , for Zn₂PP as a function of DABCO:Zn₂PP molar ratio in CH₂Cl₂.

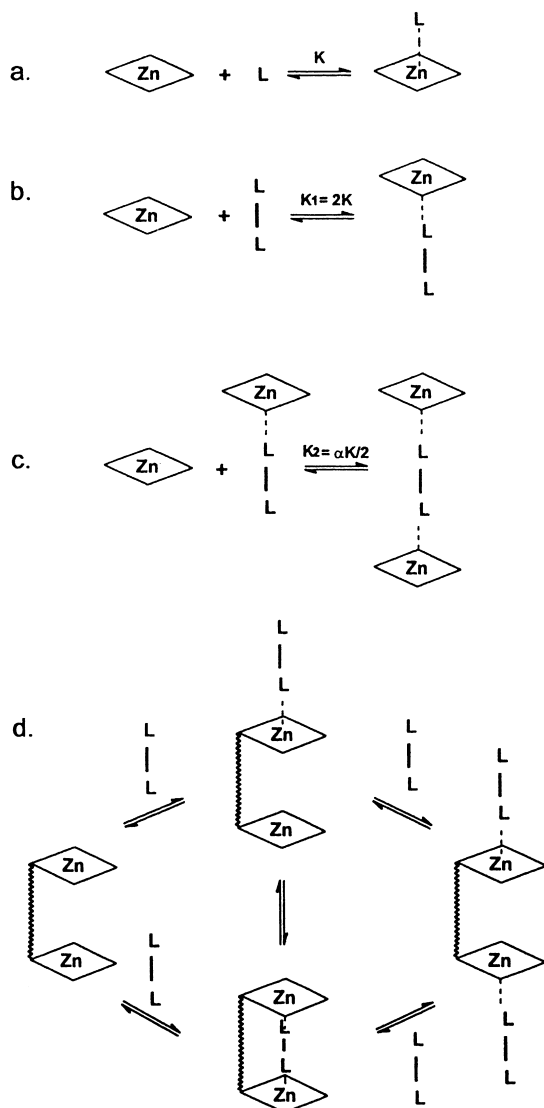
ratio of DABCO:ZnP_{phy} = 2:1 the fluorescence efficiency of ZnP_{phy} was 1.2 times that in the absence of DABCO.

The fluorescence lifetime of ZnP_{phy} in CH₂Cl₂ increased with increasing DABCO concentration from 2.7 ns in the absence of DABCO to 3.3 ns at the molar ratio DABCO:ZnP_{phy} = 5:1. Using pyridine as the solvent, the fluorescence lifetime of ZnP_{phy} was 3.7 ns. For Zn₂PP in CH₂Cl₂ at low DABCO concentrations, the fluorescence decay curves were at least two-exponential. Fitting to three-exponentials did not improve the quality of the fit. The fluorescence lifetime of the long-lived component increased from 2.5 ns in the absence of DABCO to 4.0 ns at the molar ratio DABCO:Zn₂PP = 1:1. The lifetime of the short-lived component was 1.0 ns and its proportion decreased from 8% in the absence of DABCO to 0% at molar ratios higher than DABCO:Zn₂P = 2:1. Using pyridine as the solvent, the fluorescence decay curve of Zn₂PP was one-exponential with a lifetime of 3.3 ns.

4. Discussion

A monofunctional ligand binds according to reaction **a** and a bifunctional ligand according to reaction **b** in Scheme 1. However, with a bifunctional ligand a second equilibrium is possible, leading to the formation of a 2:1 complex according to reaction **c** in Scheme 1. Both K_1 and K_2 are related by the expression $4K_2 = \alpha K_1$ where α is a measure of co-operativity between the two binding sites of the ligand (the statistical factor of 4 takes into account the degeneracy of the monobound species) [5]. Similar arguments apply to a reversed situation in which a monofunctional ligand binds to a dimeric phorbins. The situation is more complicated for an equilibrium between a bifunctional ligand and a dimer. The possible equilibria are shown by reaction **d** in Scheme 1. Not all these equilibria are important, since one of them tends to dominate [4,5]. Usually only one of the two pathways needs to be considered.

The Zn₂PP dimer molecule has a very flexible structure. Binding of a monofunctional ligand such as pyridine to Zn₂PP does not change the situation notably whereas binding of a bifunctional ligand such as DABCO between the Zn-macrocycles of the dimer could lead to a fixed



Scheme 1.

conformation. The binding energy for this process will generally not be twice that for binding the same ligand to a monomeric substrate because of the following factors [5]. (1) The chelate effect: binding of a single bifunctional ligand is entropically favored over binding two monofunctional ligands, and hence the binding constant for a multifunctional ligand is expected to be greater than the product of the binding constants for the separate binding processes. (2) Co-operativity: when one end of the ligand is bound, the nucleophilicity of the second site may be lowered, reducing its binding energy. (3) Global conformational changes: if ligand binding reduces interactions that favor a compact conformer, it is energetically unfavorable.

4.1. Co-operativity of binding

Eq. (1) can be used to determine whether there is co-operativity in the binding of the ligand [4,5,11]

$$\ln \left(\frac{A - A_0}{A_f - A} \right) = \alpha \ln[\text{free ligand}] + \ln K \quad (1)$$

where A is the absorption at a particular wavelength (λ), A_0 the initial absorption at λ , A_f the final absorption at λ , K the binding constant, and α a constant defining the number of ligands bound per site. Thus, a plot of $\ln\{(A - A_0)/(A_f - A)\}$ versus $\ln[\text{free ligand}]$, a Hill plot, should yield a straight line of a slope $\alpha = 1$ for independent, identical binding at the two sites. Positive co-operative binding in which the second binding is aided by the first one gives a slope >1 whereas negative co-operativity gives a slope <1 . The Hill plot for Zn_2PP complexed with pyridine yielded a straight line with slope $\alpha = 1.14$ up to the molar ratio of pyridine: $\text{Zn}_2\text{PP} = 40:1$. This indicates an allosteric behavior in which the first binding facilitates the second binding [11]. Allosteric behavior is usually only observed for weakly bound ligands such as pyridine [5]. For stronger ligands, the titration curves are not sensitive to a small difference between the first and second binding constants. For Zn_2PP titrated with DABCO, the slope $\alpha = 1.61$ was obtained, indicating positive co-operativity of binding and the formation of a fixed 1:1 complex in which DABCO binds both macrocycles of one Zn_2PP molecule.

4.2. Complexation with pyridine

For a monofunctional ligand binding to a monomeric substrate, the binding constant can be obtained from the titration data using the Benesi–Hildebrand plot [12–14]:

$$\frac{[S]_0}{\Delta A} = \frac{1}{K \varepsilon [L]_{\text{tot}}} + \frac{1}{\varepsilon} \quad (2)$$

where $[S]_0$ is initial concentration of the substrate, ΔA the change in absorbance at the absorption maximum of the complex, K the binding constant, ε a constant and $[L]_{\text{tot}}$ is the total concentration of the ligand. The plot of Eq. (2) for ZnP_{Phy} titrated with pyridine shows a good linear relationship, indicating the formation of a 1:1 complex (reaction **a** in Scheme 1) with a binding constant, $K = 1.5 \times 10^4 \text{ M}^{-1}$. For Zn_2PP titrated with pyridine, the situation is more complicated because also a 1:2 complex can be formed in addition to the 1:1 complex (reactions **b** and **c** in Scheme 1). In previous studies of ligand binding to dimeric zinc-porphyrins, the 1:1 and 1:2 complexes could easily be distinguished from one another, since their absorption maxima were at different wavelengths [4,5]. For the present systems, the titration curves show only smooth changes until the saturation level is reached. Thus, the binding constants of 1:1 and 1:2 complexes cannot be determined separately. However, the plot of Eq. (2) shows a good linear dependence also for Zn_2PP titrated with pyridine. This suggests independent and equal binding to both macrocycles of Zn_2PP and, hence, the obtained binding constant of $7 \times 10^3 \text{ M}^{-1}$ is an apparent one including both of the 1:1 and 1:2 complexes.

4.3. Complexation with DABCO

For the substrates ZnP_{Phy} and Zn_2PP , the binding of DABCO is clearly much stronger than the binding of pyridine as judged from the changes in the absorption spectra. This is in good agreement with the previous studies on covalently-linked zinc-porphyrin dimers [4,5]. The complexation between ZnP_{Phy} and DABCO follows reactions **b** and **c** in Scheme 1. The changes in the absorption spectrum of ZnP_{Phy} with increasing DABCO concentration reach a saturation level at the molar ratio of $\text{DABCO}:\text{ZnP}_{\text{Phy}} = 6:1$. At this molar ratio, the spectrum is identical with that obtained with pyridine at the saturation level (Fig. 2). Thus, for the ZnP_{Phy} concentration of $2\ \mu\text{M}$, the formation of the 2:1 complexes according to reaction **c** in Scheme 1 is unlikely. This is confirmed by the linear dependence of the Benesi–Hildebrand plot. The binding constant, $K_1 = 1.5 \times 10^5\ \text{M}^{-1}$ is obtained for a 1:1 complex of ZnP_{Phy} and DABCO.

For the complexation of Zn_2PP with DABCO, the saturation level for changes in the absorption spectrum is reached already at the molar ratio of $\text{DABCO}:\text{Zn}_2\text{PP} = 3:1$. If Zn_2PP would be totally complexed with DABCO and if only 1:2 complexes were present, the absorption spectrum of Zn_2PP should be similar to that obtained with pyridine at the saturation level. However, a blue shift of the Q-band is observed in the presence of DABCO and the Soret-band shifts only to 429 nm whereas in the titration with pyridine it shifts to 431 nm. This suggests the formation of 1:1 complexes at low $\text{DABCO}:\text{Zn}_2\text{PP}$ molar ratios whereas at higher molar ratios both 1:1 and 1:2 complexes are present in the solution.

When the fluorescence decay curves of Zn_2PP in CH_2Cl_2 were analyzed as a sum of two exponents, the long-lived component of 2.5 ns is close to the decay time of 2.7 ns for ZnP_{Phy} in CH_2Cl_2 . The one-exponential decay observed using pyridine as solvent suggests the absence of fluorescent impurities in the Zn_2PP . Since the spacer between the Zn-macrocycles is flexible, the molecules can exist as a mixture of conformers with a variety of orientations and distances between the Zn-macrocycles [5,15–20]. Different conformers would have slightly different spectral properties leading to a non-exponential fluorescence decay curve. Since the fluorescence lifetimes of only slightly different conformations would be very close, they cannot be resolved from the measured decay curves. Thus, although the decay curve can be analyzed with two-exponentials, this is only the lower limit of the possible fluorescing species present in the sample. In the presence of DABCO, the proportion of the short-lived component decreases and the lifetime of the long-lived component increases. This is in agreement with the increase of the relative fluorescence quantum yield ϕ_{fl} . The changes in the fluorescence data take place already at very low $\text{DABCO}:\text{Zn}_2\text{PP}$ molar ratios: the maximum value $\phi_{\text{fl}} = 0.71 \pm 0.05$ is obtained already at the molar ratio of $\text{DABCO}:\text{Zn}_2\text{PP} = 1.5:1$, and the fluorescence lifetime of

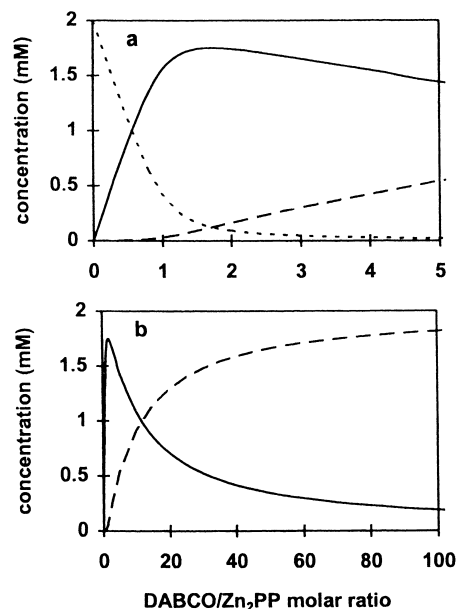


Fig. 5. The calculated concentrations for the fixed 1:1 complex (—) and the 2:1 complex (---) of Zn_2PP in CH_2Cl_2 as a function of $\text{DABCO}:\text{Zn}_2\text{PP}$ molar ratio, (a) from 0 to 5 and (b) from 0 to 100. The concentration of the uncomplexed Zn_2PP is indicated as (•••).

the long-lived component saturates at 4 ns already at the molar ratio $\text{DABCO}:\text{Zn}_2\text{PP} = 1:1$. These results are in good agreement with the relatively high value of co-operativity obtained from the Hill-plot and indicate a strong tendency to form a fixed 1:1 complex. Thus, the formation of an open 1:1 complex is neglected in the present system. With further increase in the DABCO concentration, ϕ_{fl} decreases to 0.63 ± 0.05 (Fig. 4). This indicates the formation of 1:2 complexes from the fixed 1:1 complexes: the more flexible structure of the 1:2 complexes leads to smaller ϕ_{fl} -values.

The complexation of Zn_2PP with DABCO should not follow the simple Benesi–Hildebrand relation Eq. (2). Thus, the ϕ_{fl} data was used to calculate the binding constant for the fixed 1:1 complex. However, the final state, i.e. the value of ϕ_{fl} when only fixed 1:1 complexes were present, could not be measured. The highest measured value, $\phi_{\text{fl}} = 0.71 \pm 0.05$, led to concentration values which were higher than the actual DABCO concentration. Thus, the least-squares curve-fitting routine was used to analyze the data. The values $K_1 = 1.0 \times 10^7\ \text{M}^{-1}$ and $\phi_{\text{fl}}(\text{final}) = 0.79$ were obtained. At molar ratios $\text{DABCO}:\text{Zn}_2\text{PP} \geq 1:1$, the Benesi–Hildebrand plot Eq. (2) was linear and a binding constant $K_2 = 5.0 \times 10^4\ \text{M}^{-1}$ was determined. This constant is attributed to the formation of 1:2 complexes from the fixed 1:1 complexes. These data can be used to calculate the proportions of the complexes at different DABCO concentrations. The results are shown in Fig. 5. The highest proportion, 88% for the fixed 1:1 complex is obtained at the molar ratio $\text{DABCO}:\text{Zn}_2\text{PP} = 2:1$. A very high molar ratio, $\text{DABCO}:\text{Zn}_2\text{PP} = 12:1$, is needed to reduce the proportion of the fixed 1:1 complex to 50%.

5. Conclusions

The addition of DABCO produced strong changes in the absorption and fluorescence spectra of the dimer Zn₂PP, indicating the formation of a fixed 1:1 complex where DABCO is bound between the Zn-macrocycles of the dimer. The binding constant of this complex is $1 \times 10^7 \text{ M}^{-1}$ and its proportion is highest, about 88%, at the molar ratio DABCO: Zn₂PP = 1.5:1. At higher molar ratios, a second DABCO molecule binds to the dimer breaking down the fixed complex. The binding constant of the 1:2 complex, $5 \times 10^4 \text{ M}^{-1}$ is much lower than that for the fixed 1:1 complex. Thus, the proportion of the fixed 1:1 complex persists at 10% even for molar ratios DABCO:Zn₂PP = 100:1. The developed method will be applied for fixing the conformation of the triad molecules [1]. This is essential for increasing the efficiency of photoinduced electron transfer in these systems.

Acknowledgements

We gratefully acknowledge the financial support from the Academy of Finland and the Technology Development Center of Finland to our programme of photochemistry of organic films.

References

- [1] A.Y. Tauber, J. Helaja, I. Kilpeläinen, P.H. Hynninen, *Acta Chem. Scand.* 51 (1996) 88.
- [2] A.Y. Tauber, Thesis, University of Helsinki, 1996.
- [3] C.A. Hunter, P. Leighton, J.K.M. Sanders, *J. Chem. Soc., Perkin Trans. 1* (1989) 3.
- [4] C.A. Hunter, M.N. Meah, J.K.M. Sanders, *J. Am. Chem. Soc.* 112 (1990) 5773.
- [5] H.L. Anderson, C.A. Hunter, M.N. Meah, J.K. Sanders, *J. Am. Chem. Soc.* 112 (1990) 5780.
- [6] A.V. Chernook, A.M. Shulga, E.I. Zenkevich, U. Rempel, C. von Borczykowski, *J. Phys. Chem.* 100 (1996) 1918.
- [7] P.H. Hynninen, S. Lötjönen, *Org. Magn. Reson.* 21 (1983) 757.
- [8] The synthesis of PP1, 2 will be published elsewhere.
- [9] T.H. Tran-Thi, J.F. Lipskier, P. Maillard, M. Momenteau, J.-M. Lopez-Castillo, J.-P. Jay-Gerin, *J. Phys. Chem.* 96 (1992) 1073.
- [10] N.V. Tkachenko, D. Grandell, M. Ikonen, A. Jutila, V. Moritz, H. Lemmetyinen, *Photochem. Photobiol.* 58 (1993) 284.
- [11] L. Stryer, *Biochemistry*, Freeman, New York, 1998, pp. 154–156.
- [12] H.A. Benesi, J.H. Hildebrand, *J. Am. Chem. Soc.* 71 (1949) 2703.
- [13] W.B. Person, *J. Am. Chem. Soc.* 87 (1965) 167.
- [14] D.A. Deranlau, *J. Am. Chem. Soc.* 91 (1969) 4050.
- [15] J.C. Hindman, R. Kugel, M.R. Wasielewski, J.J. Katz, *Proc. Natl. Acad. Sci.* 75 (1978) 2076.
- [16] R.R. Bucks, S.G. Boxer, *J. Am. Chem. Soc.* 104 (1982) 340.
- [17] R.R. Bucks, T.L. Netzel, I. Fujita, S.G. Boxer, *J. Phys. Chem.* 86 (1982) 1947.
- [18] C.A. Hunter, J.K.M. Sanders, *J. Am. Chem. Soc.* 112 (1990) 5525.
- [19] P. Leighton, J.A. Cowan, R.J. Abraham, J.K.M. Sanders, *J. Org. Chem.* 53 (1988) 733.
- [20] K. Maruyama, A. Osuka, *Pure Appl. Chem.* 62 (1990) 1511.